Resonant x-ray magnetoelectric effect in a centrosymmetric spinel oxide

M. Matsubara,[1,2,3] Y. Shimada,[3] K. Ohgushi,[4] T. Arima,[5] and Y. Tokura[1,3,6]

[1]*National Institute of Advanced Industrial Science and Technology (AIST), Tsukuba 305-8562, Japan*

[2]*CREST, Japan Science and Technology Agency (JST), Kawaguchi, Saitama 332-0012, Japan*

[3]*Department of Applied Physics, University of Tokyo, Tokyo 113-8656, Japan*

[4]*Institute for Solid State Physics, University of Tokyo, Kashiwa, Chiba 277-8581, Japan*

[5]*Institute of Multidisciplinary Research for Advanced Materials, Tohoku University, Sendai 980-8577, Japan*

[6]*Multiferroics Project, ERATO, Japan Science and Technology Agency (JST), ASI, RIKEN, Wako 351-0198, Japan*

We show clear evidence that the local magnetoelectric (ME) effect arising from the noncentrosymmetric magnetic sites can be element-specifically detected by using the resonant x-ray ME scattering (XMES), even in systems where the space-inversion (I) or the time-reversal (R) symmetry is globally restored. At the (222) reflection in a centrosymmetric spinel oxide $MnCr_2O_4$, where the conventional Mn-resonant x-ray magnetic scattering is forbidden, we have observed a resonant magnetic signal at the intra-atomic $1s$-$3d$ absorption edge of Mn ions on tetrahedral sites, which is uniquely attributed to the XMES. This unique x-ray scattering is caused by a transfer of the spectral weight between the electric dipole ($E1$) and electric quadrupole ($E2$) transitions through the spin-orbit coupling. The possibility of the important application utilizing the ME scattering technique is discussed as well.

PACS number(s): 75.80.+q, 75.50.Gg, 78.70.Ck

The magnets with broken space-inversion symmetry have recently been of great interest from the viewpoints of both fundamental physics and technological applications to future spintronics.[1,2] Such noncentrosymmetric magnets, including multiferroic materials, can potentially host the new functionality between magnetism and dielectricity via the magneto-electric (ME) interaction, which makes it possible to control the magnetization by electric fields and/or the polarization by magnetic fields.[3,4] Stepping out from the traditional phenomenological theory based on the magnetic point group, recent experimental and theoretical studies suggest that it is important to elucidate a more microscopic quantum mechanism of the ME effect in terms of the magnetoelectric response of the magnetic atoms which do not occupy the inversion center.[5,6] The ME effect can be observed only in the exceptional systems in which the space-inversion (I) and the time-reversal (R) symmetries are simultaneously and macroscopically broken. However, one can speculate that each magnetic element at locally I-broken sites should become a source of the ME effect. A magnetic ion in the tetrahedral ligand, as shown in Fig. 1(a), is a prototypical example. When an external magnetic field (H) is applied in the configuration shown in Fig. 1(b), a local electric dipole (p) represented by $p_i = \alpha_{ij}H_j$ can be induced.[7] The direction of p becomes reversed by the I or R operation, as shown in Figs. 1(c) and 1(d). Therefore, if a system has a global I or R symmetry, even though I and R symmetries are broken at a local site, the macroscopic ME signal ($F^{ME} = \Sigma_j f_j^{ME}$) is absent because the sum of the local amplitude (f_j^{ME}) at every ME active site is always canceled. However, if the local ME activity can be probed even in a globally I or R symmetric system, it may provide the key information for the materials design of the ME functions. When such local ME units can be accumulated in an uncanceled manner, they may lead to the potentially large macroscopic ME effect.

In this Rapid Communication, we report on a unique method to detect the locally active ME effect even in a material which has a global I or R symmetry. In the x-ray scattering [$F^{ME}(Q,\omega) = \Sigma_j f_j^{ME}(Q,\omega)e^{-iQ\cdot r_j}$], the local amplitudes are multiplied by a phase factor ($e^{i\phi} = e^{-iQ\cdot r_j}$) before summing up. With use of x-ray ME scattering (XMES) with $\phi = \pm \pi$, we have successfully observed the local ME effect and elucidated its microscopic mechanism in a centrosymmetric spinel oxide $MnCr_2O_4$. The limit of $Q = \omega = 0$ in the XMES corresponds to the ME effect, which is absent in this globally centrosymmetric compound.

The crystal structure of spinel oxides AB_2O_4 contains crystallographically distinct two cation sites, namely, tetrahedral A sites and octahedral B sites, as shown in Fig. 2(a). $MnCr_2O_4$ belongs to the normal spinel in which Mn^{2+} and Cr^{3+} ions occupy the A and the B sites, respectively. It shows ferrimagnetism between 14 and 48 K,[8] which results in the broken R symmetry. On the other hand, it has a centrosymmetric structure (space group $Fd\bar{3}m$). While the B sites
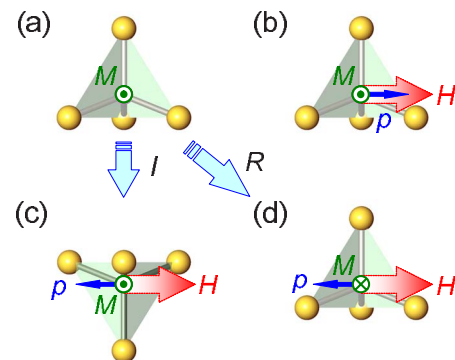
FIG. 1. (Color online) [(a) and (b)] ME effect of a magnetic ion surrounded by a tetrahedral oxygen ligand. An electric dipole (p) can be induced by an application of an external magnetic field (H) via the ME effect. The direction of p becomes reversed under (c) the space-inversion (I) or (d) the time-reversal (R) operations.
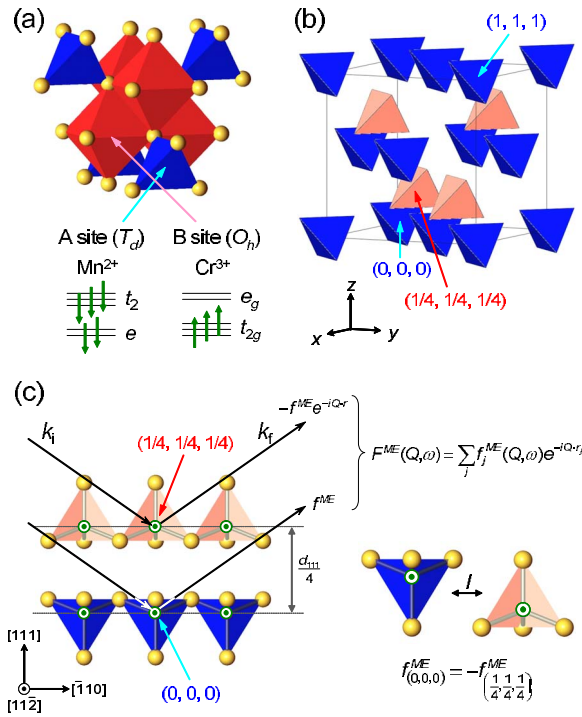
FIG. 2. (Color online) (a) The crystal structure of spinel $MnCr_2O_4$ and the electronic configurations of the Mn^{2+} and the Cr^{3+} ions, which occupy the tetrahedral A sites (T_d) and the octahedral B sites (O_h), respectively. (b) A sites in the unit cell of spinel structure. (c) The alignments of the A sites along the [111] direction. The signs of the ME scattering at the (0,0,0) and $(\frac{1}{4}, \frac{1}{4}, \frac{1}{4})$ positions are opposite.

(O_h:$m3m$) have an inversion center, the A sites (T_d:$\bar{4}3m$) do not. Therefore, the Mn^{2+} ions at the A sites become sources of the ME effect. As shown in Fig. 2(b), there are the same numbers of tetrahedra with opposite directions in the unit cell, such as two tetrahedra at (0,0,0) and $(\frac{1}{4}, \frac{1}{4}, \frac{1}{4})$. Since the magnetic moments of all the Mn^{2+} ions align in the same direction, the signs of the local ME effect (f_j^{ME}) are different at the (0,0,0) and $(\frac{1}{4}, \frac{1}{4}, \frac{1}{4})$ positions. As a result, the uniform ME signal arising from the noncentrosymmetric A sites vanishes. As mentioned above, however, the local ME effect can be detected by using XMES. As anticipated from Fig. 2(c), the XMES signal is expected to be maximized at the (222) reflection but canceled out at the (444) reflection. Up to now, the XMES has been reported in a multiferroic $GaFeO_3$ (Ref. 9) and a centrosymmetric spinel oxide Fe_3O_4 (Ref. 10) around the Fe K-absorption edge. In these cases, however, there were some difficulties to identify the XMES signal since Fe ions occupy more than one crystallographic site, that is, the Fe1 and the Fe2 sites in $GaFeO_3$ and the A and the B sites in Fe_3O_4, and therefore the complicated analyses were required. In $MnCr_2O_4$, Mn^{2+} ions only occupy the A sites. In addition, the contribution of Mn ions to the magnetic structure factor at the (222) reflection is 0 because the spin directions of all the Mn^{2+} ions are identical, as mentioned above. Therefore, the resonant magnetic signal at the (222) reflection around the Mn K-absorption edge in $MnCr_2O_4$ would clearly prove the existence of the XMES, which is
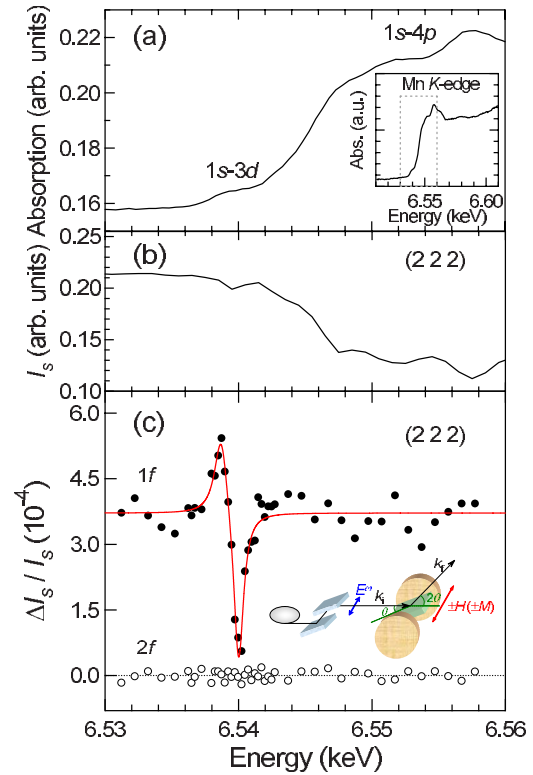
FIG. 3. (Color online) (a) X-ray absorption spectrum at room temperature; (b) x-ray scattering spectrum; and (c) magnetic field modulated x-ray scattering spectrum $\Delta I_s/I_s$ at 20 K at the (222) reflection for $E^{\omega} \| H \| [11\bar{2}]$ in the vicinity of the Mn K-absorption edge in $MnCr_2O_4$. The solid line in (c) is merely the guide for the eyes. In (c), the spectrum of the second-harmonic ($2f$) component of the magnetic modulation is also shown by open circles. The experimental configuration of the magnetic field modulated x-ray scattering is shown in the inset of (c).

quite distinct from the conventional x-ray magnetic scattering (XMS).[11] Here, we clearly show by such a case study the existence of the XMES arising from the noncentrosymmetric A site and demonstrate that the resonant XMES has great potential to investigate the microscopic mechanism of the ME effect in magnetic materials with locally lacking I symmetry.

A single crystal of $MnCr_2O_4$ with the well-developed flat (111) surfaces was grown by the chemical vapor transport method.[8] Measurements of the magnetic field modulated x-ray scattering were carried out on beamlines 1A and 16A2 at Photon Factory, KEK, Japan.[9,10] The typical energy resolution was ~2 eV. The experimental configuration is shown in the inset of Fig. 3(c). A horizontally polarized white x ray was monochromated by a Si(111) double crystal and injected on the $MnCr_2O_4$ (111) surface. The scattered x-ray intensity I_s was detected by an ionization chamber. The polarization of the incident x ray was perpendicular to the scattered plane (σ polarization) and was parallel to the external magnetic field. A modulated magnetic field with an amplitude of 800 Oe and a frequency f of 5 Hz was applied along the $[11\bar{2}]$ axis of the sample in the Voigt configuration to change periodically the magnetization direction. Then, the magnetic modulation sig-
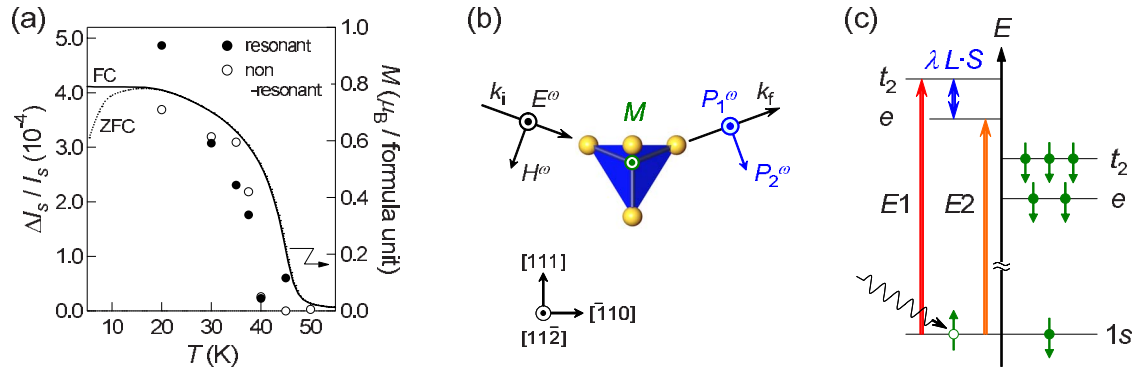
FIG. 4. (Color online) (a) Temperature dependence of the resonant (peak-to-peak) and nonresonant (background) intensities in $\Delta I_s / I_s$ at the (222) reflection around the Mn K-absorption edge. The solid and dotted lines show the magnetization in a magnetic field of 800 Oe applied along the $[11\bar{2}]$ direction. (b) The optical ME effect arising from a Mn^{2+} ion in the noncentrosymmetric A site in the configuration of $E^{\omega} \| H \| [11\bar{2}]$. (c) Microscopic origin of the XMES in $MnCr_2O_4$ (see text).

nal ΔI_s was measured with a lock-in amplifier. The ratio of ΔI_s to the total scattering intensity I_s can be approximately written in the form[9,12,13]

$$\frac{\Delta I_s}{I_s} \sim \frac{F^c \Delta F^* + F^{c*} \Delta F}{|F^c|^2}. \tag{1}$$

Here, F^c and ΔF are the structure factors for the charge and the magnetic (including the ME) scattering, respectively. As seen in Eq. (1), ΔI_s can be mainly caused by the interference terms between the charge and the magnetic scattering. Then, only the σ-polarized magnetic field modulated scattering contributes to ΔI_s because the charge scattering is σ polarized.

Figure 3(a) shows an x-ray absorption spectrum of $MnCr_2O_4$ crystal at room temperature in the vicinity of the Mn K-absorption edge. The absorption spectrum in a wider energy range is also shown in the inset of Fig. 3(a). There exist two spectral structures around 6.54 and 6.55 keV. The first weak bump is assigned to Mn $1s \rightarrow 3d$ transition (pre-edge), whereas the strong peak is assigned to Mn $1s \rightarrow 4p$ transition (main edge). A fairly large offset of the absorption mainly comes from the Cr K-absorption, which is located at around 6.0 keV.

Figures 3(b) and 3(c) show the x-ray scattering spectrum and magnetic field modulated x-ray scattering spectrum at 20 K at the (222) reflection for $E^{\omega} \| H \| [11\bar{2}]$. The structures observed in Fig. 3(b) are the same as that seen in Fig. 3(a). At the (222) reflection, the Mn-resonant x-ray scattering is zero, but the Cr-resonant one is finite, which leads to the large background of the scattering intensity. In Fig. 3(c), we clearly observed a resonant structure around the pre-edge region. When the polarization of x ray is parallel to the magnetization ($E^{\omega} \| M$) as in the present configuration, the conventional XMS relevant to the electric dipole-electric dipole ($E1$-$E1$) term is forbidden. In addition, at the (222) reflection the conventional Mn-resonant XMS arising from the electric quadrupole-electric quadrupole ($E2$-$E2$) process does not occur because the contribution of the Mn^{2+} ions to the magnetic structure factor at the (222) reflection reflects the difference of the magnetic scattering amplitudes of the Mn^{2+} ions at the

(0,0,0) and $(\frac{1}{4}, \frac{1}{4}, \frac{1}{4})$ positions and the signs of the magnetic scattering amplitudes arising from the $E2$-$E2$ process are the same at the two positions. Although the conventional resonant XMS can be in some cases observed even for forbidden reflections, it does not contribute to the σ-σ' scattering process.[14] Moreover, the observed signal is also distinguished from the anisotropy of the tensor of susceptibility (ATS) scattering induced by the magnetically induced lattice distortions such as magnetoelastic effect. The magnetoelastic effect is in principle second-order effect of the magnetization and hence appears as the second-harmonic ($2f$) component of the magnetic modulation signal. However, the $2f$ component was hardly observed in this study, as shown by open circles in Fig. 3(c). This means that the ATS scattering cannot be a source of the signal observed only in the $1f$ component of the magnetic field modulated x-ray scattering. From these reasons, the resonant signal observed here is uniquely assigned to the XMES. On the other hand, the underlying photon-energy-independent signal ($\sim 3.7 \times 10^{-4}$) stems from the nonresonant XMS due to the magnetization precession of Cr^{3+} moments by the oscillating magnetic field of x ray through the magnetic dipole-magnetic dipole ($M1$-$M1$) term. Although the typical nonresonant XMS intensities for a pure magnetic scattering are from 10^{-6} to 10^{-8} compared to the charge scattering, this value can become larger when the charge-magnetic interference takes place in a ferromagnet (ferrimagnet), as in the present case.[9,10]

In Fig. 4(a), we show temperature dependence of the intensities of the resonant (peak-to-peak) and nonresonant (background) components in $\Delta I_s / I_s$ at the (222) reflection. The temperature variations of both components are parallel to that of the magnetization in a magnetic field of 800 Oe applied along the $[11\bar{2}]$ direction. The resonant XMES reflects the average magnetization of Mn^{2+} ions at the A sites. On the other hand, the nonresonant XMS selectively detects the magnetization of Cr^{3+} ions at the B sites because the contribution of Mn^{2+} ions is absent at the (222) reflection. Thus, the site-selective measurement of the magnetization is possible by using the resonant XMES which comes from the ME effect at the noncentrosymmetric A sites and the nonresonant XMS from the magnetization precession at the B sites, respectively.

The XMES corresponds to the x-ray version of the ME effect. As shown in Fig. 4(b), by application of oscillating magnetic field (H^ω) of light, an oscillating electric polarization (P^ω) is induced via the optical ME effect, which is expressed as $P_i^\omega = \alpha_{ij}(\omega)H_j^\omega$.[15] Microscopically, the optical ME effect originates from the electric dipole-magnetic dipole ($E1$-$M1$) or the electric dipole-electric quadrupole ($E1$-$E2$) term.[16,17] Because the $M1$ transition intensity is small in the x-ray region, the $E1$-$E2$ term mainly contributes to the optical ME effect.[18] The coefficient $\alpha(\omega)$ can be resonantly enhanced at the photon energy where the $E1$- and the $E2$-allowed states hybridize through the spin-orbit coupling. In fact, the observed XMES spectrum can be interpreted with the $E1$-$E2$ interference model based on a MnO_4 cluster.[10,18] As shown in Fig. 4(c), Mn $3d$ states are split into e and t_2 states in a tetrahedral (T_d) crystal field. All the orbitals are only occupied by majority-spin electrons. Because of the lack of the I symmetry in the T_d crystal field, t_2 states are hybridized with $4p$ states. Then, the $E1$ transition is partially allowed from Mn $1s$ to t_2 states, while the $E2$ transition is allowed from Mn $1s$ to e states.[10] The XMES is caused by a transfer of the spectral weight between the $E1$ and the $E2$ transitions through the spin-orbit coupling ($\lambda L \cdot S$) between the e and t_2 states. As a result, the crystal field splitting energy ($10Dq$) between the e and t_2 states will show up as the splitting width (~ 1.3 eV) in the dispersion-type resonant XMES signal in Fig. 3(c). Though the observed resonant XMES signal in $MnCr_2O_4$ is $\sim 5 \times 10^{-4}$ at the pre-edge region, the resonant part of $\Delta I_s / I_s$ for the Mn $1s$-$3d$ transition (excluding the large background from the Cr K absorption) reaches $\sim 1\%$, which is consistent with the value observed in Fe_3O_4.[10] Thus, the XMES spectroscopy can probe the local ME unit and, hence, has a great advantage to elucidate a microscopic mechanism of the ME effect for a broad range of materials with potential ME structural units.

Recently, Igarashi and Nagao[19] numerically calculated the intensity difference of the resonant x-ray scattering between two opposite directions of the applied magnetic field for spinel oxides. They obtained the dispersion-type resonant structure at the (222) reflection around the pre-edge region of Mn K absorption in $MnCr_2O_4$. Its spectral shape and strength are similar to the XMES spectrum observed here. This theoretical analysis also supports our conclusion.

The present element-specific resonant XMES spectroscopy also gives a method to investigate the spin arrangements at the noncentrosymmetric sites and, therefore, may provide a valuable clue to the magnetic state in the interfaces and the junctions of the magnetic superlattices. In addition, the ME scattering technique is also applicable for the periodic array of the noncentrosymmetric-shape magnets ranging from a nanometer to millimeter scale by using electromagnetic waves with wavelengths corresponding to the sizes of the periodic structures, which are of growing interest.[20,21]

In summary, we have clearly shown the existence of the XMES distinct from the conventional XMS. We have observed the resonant XMES signal at the $1s$-$3d$ absorption edge of Mn ions on tetrahedral sites in a globally centrosymmetric spinel oxide $MnCr_2O_4$ and demonstrated that the resonant XMES can probe the local ME effect at the noncentrosymmetric A site. The resonant XMES, with element- and site-specific characteristics, has a great advantage of elucidating a microscopic quantum mechanism of the ME effect, and it is a unique way to detect the local ME effect at the noncentrosymmetric sites in the systems where I or R symmetry is globally restored. Moreover, the XMES technique may give a new possibility of a powerful detection method of toroidal moments,[9,22] which has been discussed as an important factor of the microscopic mechanism of the ME effect.

---

[1] T. Kimura, T. Goto, H. Shintani, K. Ishizaka, T. Arima, and Y. Tokura, Nature (London) **426**, 55 (2003).

[2] Th. Lottermoser, T. Lonkai, U. Amann, D. Hohlwein, J. Ihringer, and M. Fiebig, Nature (London) **430**, 541 (2004).

[3] N. A. Spaldin and M. Fiebig, Science **309**, 391 (2005).

[4] M. Fiebig, J. Phys. D **38**, R123 (2005).

[5] H. Katsura, N. Nagaosa, and A. V. Balatsky, Phys. Rev. Lett. **95**, 057205 (2005).

[6] M. Mostovoy, Phys. Rev. Lett. **96**, 067601 (2006).

[7] R. R. Birss, *Symmetry and Magnetism* (North-Holland, Amsterdam, 1966).

[8] K. Ohgushi, Y. Okimoto, T. Ogasawara, S. Miyasaka, and Y. Tokura, J. Phys. Soc. Jpn. **77**, 034713 (2008).

[9] T. Arima, J. H. Jung, M. Matsubara, M. Kubota, J. P. He, Y. Kaneko, and Y. Tokura, J. Phys. Soc. Jpn. **74**, 1419 (2005).

[10] M. Matsubara, Y. Shimada, T. Arima, Y. Taguchi, and Y. Tokura, Phys. Rev. B **72**, 220404(R) (2005).

[11] M. Blume, J. Appl. Phys. **57**, 3615 (1985).

[12] K. Namikawa, M. Ando, T. Nakajima, and H. Kawata, J. Phys.

Soc. Jpn. **54**, 4099 (1985).

[13] C. Vettier, D. B. McWhan, E. M. Gyorgy, J. Kwo, B. M. Buntschuh, and B. W. Batterman, Phys. Rev. Lett. **56**, 757 (1986).

[14] M. Blume, *Resonant Anomalous X-ray Scattering, Theory and Applications* (Elsevier Science, Amsterdam, 1994).

[15] Only the σ-polarized ($\parallel[11\bar{2}]$) component contributes to the magnetic modulation signal ΔI_s in the present case.

[16] L. D. Barron and J. Vrbancich, Mol. Phys. **51**, 715 (1984).

[17] E. B. Graham and R. E. Raab, Philos. Mag. B **66**, 269 (1992).

[18] M. Kubota, T. Arima, Y. Kaneko, J. P. He, X. Z. Yu, and Y. Tokura, Phys. Rev. Lett. **92**, 137401 (2004).

[19] J. Igarashi and T. Nagao, J. Phys. Soc. Jpn. **77**, 084706 (2008).

[20] N. Kida, T. Yamada, M. Konoto, Y. Okimoto, T. Arima, K. Koike, H. Akoh, and Y. Tokura, Phys. Rev. Lett. **94**, 077205 (2005).

[21] M. Konoto, T. Yamada, Koike, H. Akoh, T. Arima, and Y. Tokura, J. Appl. Phys. **103**, 023904 (2008).

[22] B. B. Van Aken, J.-P. Rivera, H. Schmid, and M. Fiebig, Nature (London) **449**, 702 (2007).